



## DEVELOPING RELATIONSHIP TO PREDICT THE IMMERSION CORROSION RATE OF HVOF SPRAYED IRON BASED AMORPHOUS METALLIC COATING ON 316 STAINLESS STEEL

\*Vignesh S<sup>1</sup>, Shanmugam K<sup>2</sup>, Balasubramanian V<sup>3</sup>, Sridhar K<sup>4</sup> and Kamal Jayaraj R<sup>5</sup>

<sup>1,5</sup>Research Scholar, <sup>2</sup>Associate Professor and <sup>3</sup>Professor, Centre for Materials Joining and Research (CEMAJOR), Department of Manufacturing Engineering, Annamalai University, Annamalai Nagar – 608 002, Tamil Nadu, India.

<sup>4</sup>Scientist, Naval Materials Research Laboratory (NMRL), Ambernath Thane-421506, Maharashtra, India.

### ABSTRACT

Fluid handling equipment such as propellers, impellers, pumps possess the inherent risk of flow-dependent erosion-corrosion problems. Iron based amorphous coatings exhibit high erosion-corrosion resistance. High velocity oxy-fuel spray process is widely used to deposit erosion-corrosion resistance amorphous coatings. In this investigation, iron based amorphous metallic coating was deposited on 316 stainless steel using HVOF spray process by optimized process parameters such as oxygen flow rate, fuel flow rate, powder feed rate, carrier gas flow rate, and spray distance. The immersion corrosion test was conducted to evaluate the corrosion rate of uncoated and iron based amorphous coated SS by varying the corrosion test parameters such as pH value, chloride ion concentration and immersion time. Empirical relationships were established to predict the corrosion rate of uncoated and iron based amorphous coated 316 SS. The corrosion morphology of the uncoated and coated samples was done by scanning electron microscope. From the results, it is found that, pH value appeared to be the most significant parameters affecting the corrosion properties of the iron based amorphous coating.

*Key words:* High velocity oxy fuel spray, Iron based amorphous metallic coating, Corrosion rate.

### 1. Introduction

Marine components such as propellers, pumps and impellers experienced the corrosion problems every year. Stainless steels are widely used to make many of the marine components because of its capability of resist hazardous corrosion, erosion and abrasion damages [1]. Of these, AISI 316L stainless steel provides good corrosion resistance under solid particle and slurry based impingement conditions, because of rich content of chromium oxide passive film which resist the surface destructions even in rapid fluid flow and higher temperature conditions (up to 60<sup>0</sup> C) [2, 3].

Corrosion attack occurs on top surfaces and critical sections of the components which are affected by high velocity of fluid flow and slurry impingements. Recently, many researchers [4, 5] have attempted various coatings on the stainless steel substrate and these coatings include metallic, non metallic and ceramics coatings. Even though, organic coatings are cost effective and used in limited applications, they exhibit less corrosion resistance. Advanced corrosion resistance and better binding strength of metallic and ceramics coatings grab more interest in corrosion field.

It is understood from the literature that ceramic coatings, thermally sprayed WC/Co-Cr and WC coatings are predominantly used for improving corrosion resistance.

Recently, a new kind of thermally sprayed iron based amorphous metallic coatings (AMCs) were developed with low cost and high hardness [6]. The fabrication of amorphous coatings requires fast cooling rate to prevent formation of nucleation and nucleation growth. Due to this, the microstructure of coating does not contain any crystalline grains and grain boundaries and found that the sizes of crystallites are in nano scales [7].

One of the ways to achieve the above is to employ thermal spraying techniques like high velocity oxy-fuel (HVOF) spray, twin wire arc spraying (TWAS) and atmospheric plasma spraying (APS) to deposit metallic glass coatings (MGCs). It is evident from the literature [8-10] that the TWAS and APS coatings are resulted in problems such as oxide inclusions, poor interlamellar bonding, high porosity, etc. However, HVOF spray process can produce coatings with

\*Corresponding Author - E- mail: vignesh\_phd@yahoo.co.in

minimum oxide inclusion, high amorphicity, high hardness and less porosity compared to APS and TWAS processes. It is understood from the literature review that HVOF sprayed iron based amorphous metallic coatings on stainless steel are very scant. Moreover, there is no information available to predict the corrosion rate of the HVOF sprayed iron based amorphous coatings on 316 SS.

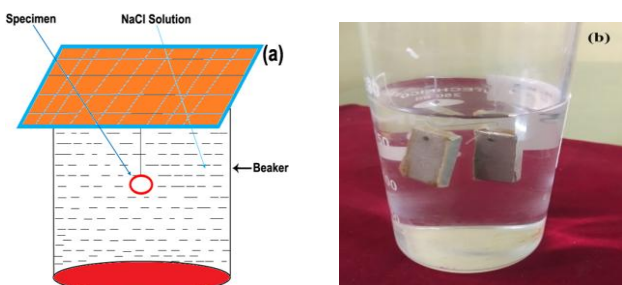
Hence in this investigation, an attempt has been made to predict the immersion corrosion rate of HVOF sprayed iron based amorphous metallic coating on naval grade AISI 316 stainless steel substrates by developing an empirical relationship incorporating, chloride ion concentration, pH value and immersing time.

## 2. Experimental procedure

AISI 316 stainless steel was used as the substrate material for the coatings and the substrates were grit blasted and subjected to ultrasonic cleaning prior to obtain good coating deposition. An in-house high velocity oxy-fuel spray system was used to obtain the iron based amorphous coatings. The HVOF process parameters used in this investigation was taken from previous study [11]. The HVOF spraying parameters, presented in Table 1, were used to deposit the coatings.

**Table 1. Optimized HVOF spray parameters used to coat iron based alumina coatings**

Parameters	Unit	Values
Oxygen flow rate	lpm	255
Fuel flow rate	lpm	58
Spray distance	mm	224
Powder feed rate	gpm	30
Carrier gas flow rate	lpm	12



**Schematic diagram of test set up**

**Photograph of test set up**

**Fig. 1 Details of immersion corrosion test.**

### 2.1 Immersion corrosion test

Immersion test was employed to evaluate the corrosion behavior of uncoated and coated samples in NaCl solution at different chloride ion concentrations, pH value and exposure time. The immersion corrosion test photographs are shown in Fig.1.

### 2.2 Finding the limits of corrosion test parameters

From the previous studies [12, 13] the predominant factors that have a greater influence on the corrosion rate of thermal sprayed coatings 316 stainless steel has been identified. They are (i) the pH value of the solution, (ii) the chloride ion concentrations of the solution, and (iii) the exposure time. From previous studies, the range of factors influencing the corrosion attack was taken and it is given in Table 2.

### 2.3 Developing the experimental design matrix

Owing to a wide range of factors, the use of three factors and central composite rotatable design matrix was chosen to minimize the number of experiments. Design matrix consisting 20 sets of coded conditions (comprising a full replication three factorial of 8 points, six corner points and six centre points) was chosen in this investigation. Table 2 presents the ranges of factors considered, and Table 3 shows the 20 sets of coded and actual values used to conduct the experiments.

For the convenience of recording and processing experimental data, the upper and lower levels of the factors were coded here as +1.682 and -1.682 respectively. The coded values of any intermediate value could be calculated using following relationship.

$$X_i = 1.682[2X - (X_{max} + X_{min})] / (X_{max} - X_{min}) \quad (1)$$

where,

$X_i$  is the required coded value of a variable  $X$  and  $X$  is any value of the variable from  $X_{min}$  to  $X_{max}$ ;

$X_{min}$  is the lower level of the variable;

$X_{max}$  is the upper level of the variable.

**Table 2. Important factors and their levels of immersion corrosion test**

S. No	Factor	Levels				
		-1.682	-1	0	+1	+1.682
1	pH value	3	4.82	7	10.18	12
2	Cl <sup>-</sup> ion conc. (M)	0.82	1.50	2.5	3.5	4.18
3	Exposure time (h)	360	490	680	870	1000

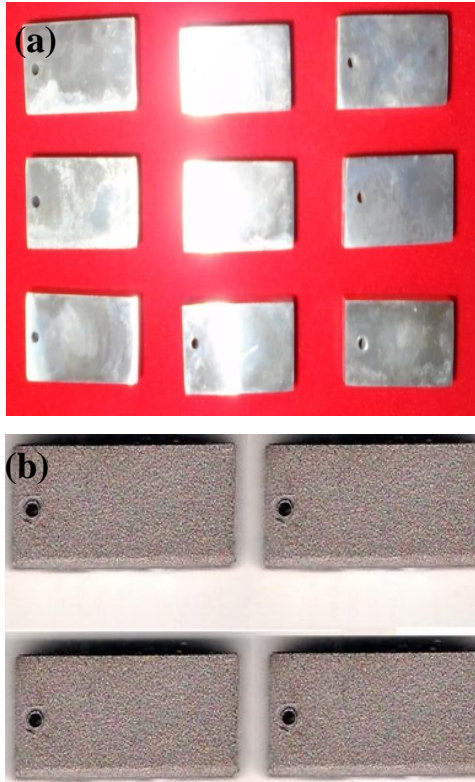


**Fig. 2 Photographs of (a) uncoated and (b) coated specimens used for immersion corrosion test**

**2.4 Recording the responses (Corrosion rate evaluation)**

The specimens were treated with metallographic polishing prior to each experiment, followed by washing in distilled water and acetone, and finally dried in warm air. The original weight ( $w_o$ ) of the specimen was recorded. Solutions of NaCl with concentrations of 0.82M, 1.50M, 2.5M, 3.5M, and 4.18M were prepared. The pH values of the solutions were maintained at pH 3, pH 4.82, pH 7, pH 10.18 and pH 12 with concentrated HCl for the acidic condition, and NaOH for the alkaline condition. The pH value was measured using a digital pH meter. The specimen was immersed in the solution of NaCl for different exposure times of 360, 490, 680, 870 and 1000 h. Finally, the corrosion products were removed by immersing the corroded specimens in a solution containing 20 g antimony trioxide ( $Sb_2O_3$ ) and 50 g stannous chloride ( $SnCl_2$ ) in 1000 ml of hydrochloric acid for five minutes. Then the specimens were washed with distilled water, dried and weighed again to obtain the final weight ( $w_1$ ).

The weight loss measurements were used to determine the corrosion rate of uncoated and HVOF

sprayed coatings 316 stainless steel under immersion corrosion tests. The weight loss ( $w$ ) is measured using the relation given by Eqn. 2,

$$w = (w_o - w_1) \tag{2}$$

Where,

$w$  = weight loss in gm.

$w_o$  = original weight before test in gm.

$w_1$  = final weight after test in gm.

The corrosion rate of uncoated and coated specimens could be calculated by using the following equation by conducting the immersion test as per the ASTM standard G31 [14],

$$Corrosion\ rate\ (CR) = \frac{87.6 \times W}{A \times D \times T} \tag{3}$$

where,

$w$  = weight loss in gm,

$A$  = surface area of the specimen in  $cm^2$

$D$  = density of the uncoated and coated samples

(Density of the coated sample was calculated using Archimedes' Method)

$T$  = Exposure time in hours

Cross sections of coatings and the corroded surfaces were investigated using scanning electron microscopy (SEM).

**Table 3. Design matrix and experimental results of immersion corrosion test**

Expt No	Original value			Corrosion rate (mm/yr)	
	pH	Cl <sup>-</sup> (M)	Time (h)	316 stainless steel	Iron based amorphous coating
1	4.82	1.5	490	0.0045	0.0015
2	10.18	1.5	490	0.0015	0.0008
3	4.82	3.5	490	0.0062	0.0021
4	10.18	3.5	490	0.0028	0.0009
5	4.82	1.5	870	0.0049	0.0016
6	10.18	1.5	870	0.0019	0.0006
7	4.82	3.5	870	0.0071	0.0024
8	10.18	3.5	870	0.0036	0.0012
9	3	2.5	680	0.0085	0.0028
10	12	2.5	680	0.0014	0.0005
11	7	0.82	680	0.0022	0.0007
12	7	4.18	680	0.0051	0.0017
13	7	2.5	360	0.0085	0.0031
14	7	2.5	1000	0.0056	0.0019
15	7	2.5	680	0.0069	0.0023
16	7	2.5	680	0.0071	0.0025
17	7	2.5	680	0.0070	0.0023
18	7	2.5	680	0.0069	0.0022
19	7	2.5	680	0.0071	0.0025
20	7	2.5	680	0.0068	0.0024

### 2.4 Developing an empirical relationship

In the present investigation, to correlate the immersion test parameters and the corrosion rate of uncoated substrate and HVOF sprayed iron based amorphous coatings on AISI 316 stainless steel, a second order quadratic model was developed. The response (corrosion rate) is a function of pH value (P), chloride ion concentration (C) and exposure time (T) and it can be expressed as,

$$\text{Corrosion rate}(CR) = f(P, C, T) \quad (4)$$

The empirical relationship must include the main and interaction effects of all factors and hence the selected polynomial is expressed as follow:

$$Y = b_0 + \sum b_i x_i + \sum b_{ii} x_i^2 + \sum b_{ij} x_i x_j \quad (5)$$

For three factors, the selected polynomial can be expressed as

$$\begin{aligned} \text{Corrosion rate}(CR) = & b_0 + b_1(P) + b_2(C) + b_3(T) + \\ & b_{11}(P^2) + b_{22}(C^2) + b_{33}(T^2) + b_{12}(PC) + b_{13}(PT) \\ & + b_{23}(CT) \end{aligned} \quad (6)$$

where  $b_0$  is the average of responses (corrosion rate) and  $b_1, b_2, b_3, \dots, b_{11}, b_{12}, b_{13}, \dots, b_{22}, b_{23}, b_{33}$ , are the coefficient that depend on the respective main and interaction factors, which are calculated using the expression given below,

$$B_i = \sum (X_i, Y_i) / n \quad (7)$$

where, 'i' varies from (1 to n) in which  $X_i$  is the corresponding coded value of a factor and  $Y_i$  is the corresponding response output value (corrosion rate) obtained from the experiment and 'n' is the total number of combination considered. All the coefficients were obtained applying central composite rotatable design matrix using the Design Expert statistical software package. After determining the significant coefficients (at 95% confidence level), the final relationship was developed including only these coefficients. The final empirical relationship obtained by the above procedure to estimate the corrosion rate of uncoated is given in eqn. (8) and HVOF sprayed iron based amorphous coatings on AISI 316 stainless steel is given in eqn. (9),

$$\begin{aligned} \text{Corrosion rate}(CR) = & \{8.51 - 1.62(P) + 8.62(C) + \\ & 3.06(T) - 1.125(PC) - 1.250(PT) + 1.125(CT) - \\ & 1.540(P^2) - 1.717(C^2) - 1.204(T^2)\} \text{mm/year} \end{aligned} \quad (8)$$

$$\begin{aligned} \text{Corrosion rate}(CR) = & \{2.81 - 5.21P\} + 2.76(C) + \\ & 8.58(T) - 8.75(PC) - 3.75(PT) + 8.75(CT) - 4.928(P^2) - \\ & 5.635(C^2) - 3.868(T^2)\} \text{mm/year} \end{aligned} \quad (9)$$

### 3. Checking the adequacy of the model

In this investigation, analysis of variance (ANOVA) is used to check the adequacy of the developed empirical relationships [15]. ANOVA test results of the responses are presented in Table 4. The adequacy of the model was tested using the ANOVA technique. In this study, the model F value and the associated probability values are checked to confirm the significance of the empirical relationships. Further, using the F-values, the predominant factors which have the major and minor effects on the responses could be assessed. From the F value assessment, it was found that the predominant factors which have direct influence on the response.

**Table 4. ANOVA test results for responses of uncoated and HVOF sprayed iron based amorphous coatings on 316 stainless steel**

Source	Uncoated 316 stainless steel		Iron based Amorphous coated 316 stainless steel	
	F value	p-value Prob > F	F value	p-value Prob > F
<b>Model</b>	10967.68	< 0.0001	373.38	< 0.0001
<b>P</b>	27385.22	< 0.0001	918.96	< 0.0001
<b>C</b>	7742.09	< 0.0001	258.73	< 0.0001
<b>T</b>	976.11	< 0.0001	24.88	0.0005
<b>PC</b>	77.18	< 0.0001	15.13	0.0030
<b>PT</b>	0.95	0.3520	2.78	0.1264
<b>CT</b>	77.18	< 0.0001	15.13	0.0030
<b>P<sup>2</sup></b>	26053.4	< 0.0001	864.79	< 0.0001
<b>C<sup>2</sup></b>	32378.08	< 0.0001	1130.74	< 0.0001
<b>T<sup>2</sup></b>	15928.11	< 0.0001	532.61	< 0.0001
<b>Lack of Fit</b>	4.785		3.21	
<b>Std. Dev.</b>	3.622		3.20	
<b>Mean</b>	5.47		1.83	
<b>R<sup>2</sup></b>	0.9999		0.9970	
<b>Adj.R<sup>2</sup></b>	0.9998		0.9944	
<b>Pred.R<sup>2</sup></b>	0.9996		0.9799	

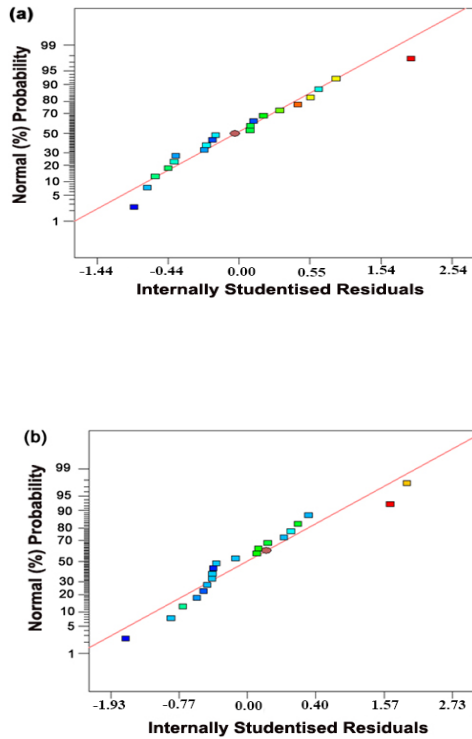


**Fig. 3 Normal probability plots for the response (a) uncoated 316 stainless steel and (b) iron based amorphous coated 316 stainless steel**

The determination coefficient ( $R^2$ ) indicates the goodness of fit for the model. In all the cases, the value of the determination coefficient ( $R^2 > 0.99$ ) indicates that less than 1% of the total variations are not explained by the empirical relationships. The value of the adjusted determination coefficient is also high, which indicates the high significance of the empirical relationships. The predicted  $R^2$  values also show good agreement with the adjusted  $R^2$  values. Adequate precision compares the range of the predicted values at the design points with the average prediction error. At the same time, a relatively low value of the coefficient of variation indicates the improved precision and the reliability of the conducted experiments. The value of probability  $> F$  in Table 4 for the empirical relationships are less than 0.05, which indicates that the empirical relationships are significant.

The Values of iron based amorphous coatings on 316 stainless steel greater than 0.1000 indicate the relationship terms are not significant. Lack of fit was not significant for all the developed empirical relationships as desired. The normal probability plots for the responses are shown in Fig. 3. From the Figure, it could be inferred that the residuals were falling on the straight line, which meant that the errors were

distributed normally [16]. Collectively, these results indicate the excellent capability of the regression model. Further, each observed value matches its experimental value well, as shown in Fig. 4.

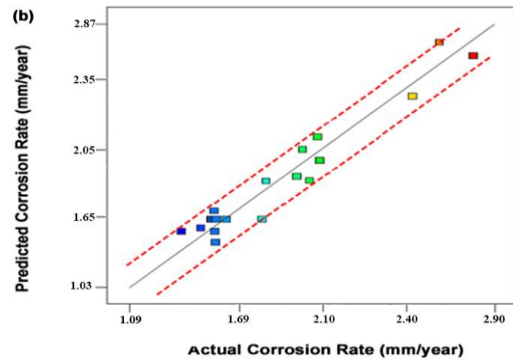


**Fig. 4 Correlation plots for the response (a) uncoated 316 stainless steel and (b) iron based amorphous coated 316 stainless steel**

#### 4. Results and discussion

The important results and discussion of the corrosion behavior of the 316 stainless steel and HVOF sprayed iron based amorphous coatings on 316 stainless steel were presented in this chapter. It clearly discusses the influence of the pH value, chloride ion concentration and exposure time on the corrosion rate and microstructural changes during the immersion corrosion tests. Most of the corrosion tests are done with a specific objective. The corrosion resistance of the materials can be determined through the rate, value and reliability of the data.

Precise results and qualitative comparisons are required. In any case, the reliability of the corrosion test is no better than the thinking and planning involved. Well-planned and executed tests reveal the reproducibility and reliability of the corrosion rate. The economical or acceptable corrosion rate depends on many factors, including cost. The important point is that the corrosion test should produce data suitable for the intended application. The closer the test corresponds to the actual application, the more reliable is the result.

##### 4.1 Effect of pH value on corrosion rate

Fig.5 shows the influence of pH on corrosion behavior of 316 stainless steel and HVOF sprayed iron based amorphous coatings on AISI 316 stainless steel in NaCl solution. In order to study the effect of pH, the

chloride ion concentration and exposure time was kept constant at 2.5 M, 680 h while the pH was varied from 3-12. From this Figure, it could be inferred that if the pH value increases, the corrosion rate decreases.

At every chloride ion concentration and time, the 316 stainless steel and iron based amorphous coated 316 stainless steel samples usually exhibited a decrease in corrosion rate with the increase in pH. The highest corrosion rate was observed at pH 3 and at neutral pH, the corrosion rate was remained constant approximately and comparatively low corrosion rate was observed in alkaline solution. It was seen that the influence of pH was more at higher concentration as compared to lower concentration in neutral and alkaline solutions [17].

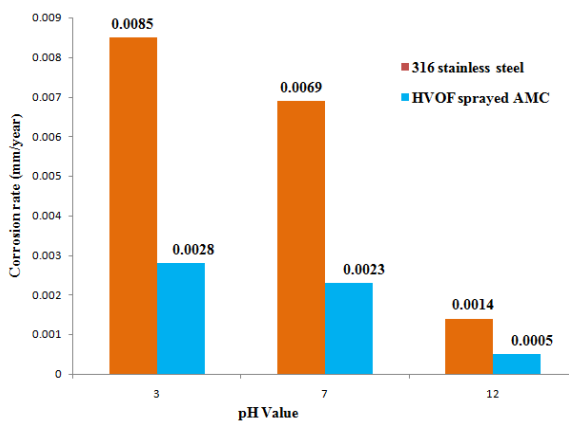


Fig. 5 Effect of pH on corrosion rate

At lower pH values, the uncoated 316 stainless steel and iron based amorphous coatings exhibited a rise in corrosion rate with an increase in chloride ion concentration. But the quantity of this rise was different in such a way that, the change in chloride ion concentration at lower concentrations affected the corrosion rate much more as compared to that of higher concentration. It shows that the increase in chloride ion concentration, the increasing rate at corrosion rate decreased that is, the influence of chloride ion concentration was much lower at higher concentrations.

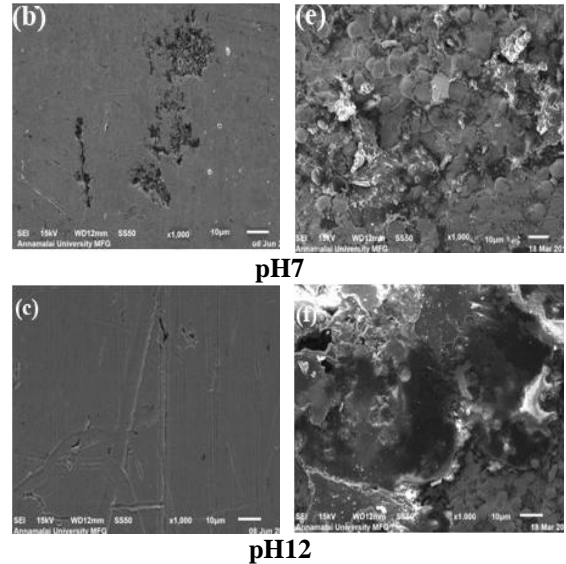
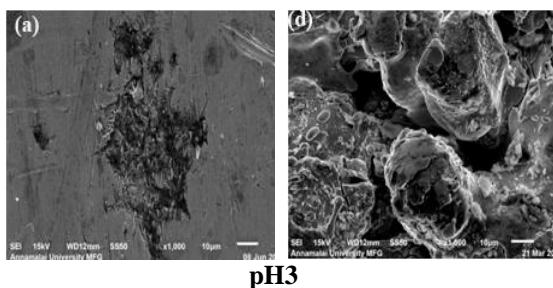


Fig. 6 Effect of pH value on corrosion behavior of uncoated (a,b&c) and HVOF sprayed iron based amorphous coated specimens (d,e&f) after immersion corrosion test in NaCl solution

From Fig.5, it can be seen that the highest corrosion rate is observed at a pH of 3. As can be expected for active metals, the rate of corrosion of these metallic materials in an acidic medium is relatively high, compared to that in neutral and alkaline solutions. In an alkaline medium, there is a formation of a barrier layer, which is insoluble in the alkaline solution and hence, a lesser corrosion rate. In acidic solutions, the barrier layer formed is completely soluble, and hence, relatively high corrosion rates are recorded in acidic solutions. In neutral solutions, the barrier layer is partially soluble. The SEM micrographs of the corroded specimens as can be seen in Fig.6. From SEM images, it was found that at higher pH values, pit corrosion has been observed only at the edges of the surface and also several small corrosion pits formed on the surface of the 316 stainless steel (Fig.6). Nevertheless it still suffered much less corrosive attack when compared to 316 stainless steel specimen at lower pH values (Fig. 6(a)).

It can be seen from Fig.6(d), at lower pH values, the iron based amorphous coated specimen which suffered a severe chemical dissolution in exposed area and the coating flaked-off in a few regions. The coating at the interface was not stable in this acidic electrolyte, and was found to have been damaged at localized regions. Thus, the substrate underneath the coating was exposed to the electrolyte. The flake-off of larger coating areas in acidic solutions was caused possibly by hydrogen gas evolution and the formation of

corrosion products after the acidic solution reaches the interface between the coating and the substrate, because the quick increase of pressure and/or volume in the limited space of the pores caused high stresses.

In the NaCl solution of pH 7, there was no pronounced corrosion damage on the surface of the coated specimen.

**4.2 Effect of chloride ion concentration on corrosion rate**

Fig.7 displays the effect of chloride ion concentration on the corrosion rate of the uncoated and iron based amorphous coatings on 316 stainless steel during the immersion corrosion tests with the pH value 7 and exposure time of 680 h. From the Figure, it could be inferred that, the corrosion rate increased on increasing the chloride ion concentration of the NaCl solutions. The highest corrosion rate is observed at the chloride ion concentration of 4.1M. It shows that the corrosion rate is increased with the increase in the chloride ion concentration.

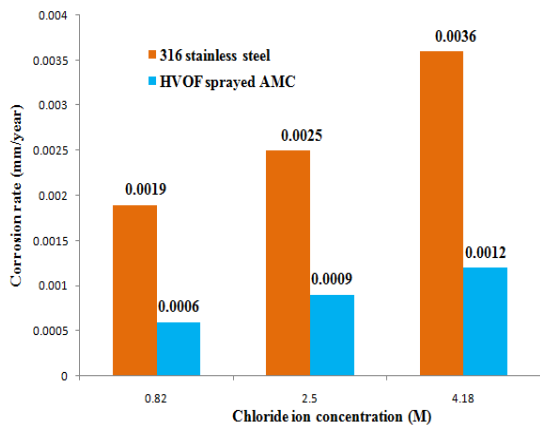


**Fig. 7 Effect of chloride ion concentration on corrosion rate**

Fig.8 reveals the SEM micrographs of the corroded specimens with different chloride ion concentrations. From the Fig.8(a), it can be seen that at lower chloride ion concentration, less corrosion pits were formed on the surface of the AISI 316 stainless steel. If the chloride ion concentration was increased, some obvious pits appeared on the surface of the specimen as represented in Fig.8(c). The alloy exhibited a rise in corrosion rate with increase in Cl<sup>-</sup> concentration and thus the change of Cl<sup>-</sup> concentration affected the corrosion rate much more in higher concentration solutions than that in lower concentration solutions. When more Cl<sup>-</sup> in NaCl solution promoted the corrosion, the corrosive intermediate (Cl<sup>-</sup>) would be rapidly transferred through the outer layer and reached

the substrate of the alloy surface. Hence, the corrosion rate was increased [18].

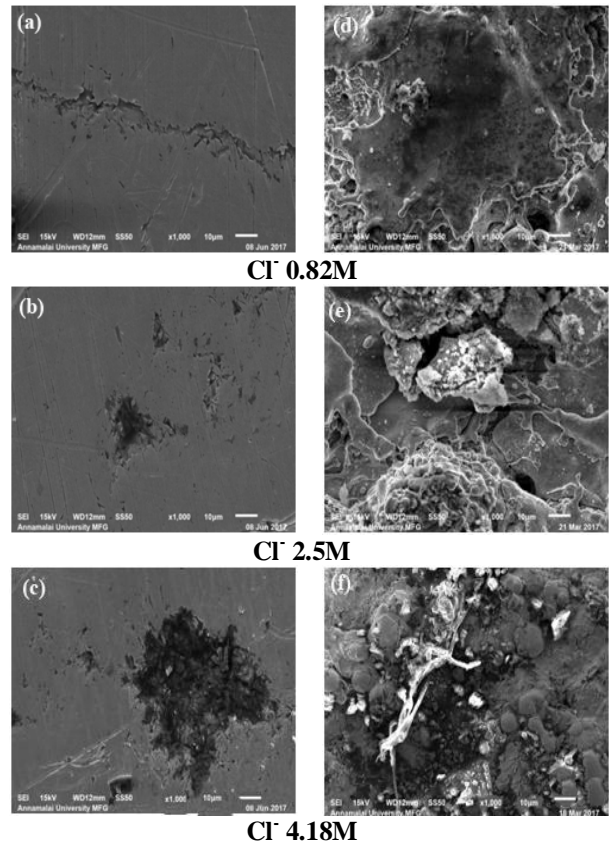


**Fig. 8 Effect of chloride ion concentration on corrosion behavior of uncoated (a,b & c) and HVOF sprayed iron based amorphous coated specimens (d,e&f) after immersion corrosion test in NaCl solution**

As shown in the SEM images Fig.8(d), it is also observed that at lower chloride ion concentrations, coating has no pronounced deterioration in this condition. At this immersion stage, because the pores and defects were not interconnecting and chloride ion concentration in 0.82M of NaCl solution was low, the corrosive electrolyte permeated slowly into the coating through these intrinsic defects. In lower chloride ion concentration solutions (0.82M of NaCl), because the corrosive electrolytes are too mild to break down the coatings, the corrosion deterioration of coated specimens was dictated by the degradation of coatings especially in inner regions of the coating. Therefore, due to the denser and more compact inner layer in the iron based amorphous coating was superior and the corrosion deterioration was slower in mild corrosive electrolytes.

In the more concentrated electrolytes (4.1M of NaCl), however, the permeation of higher concentration of chloride ions into the coating/substrate interface induced the quick breakdown of coatings and caused a localized damage on the underneath stainless steel substrate (Fig.8(f)). With the initiation of localized corrosion, high stresses were developed as a consequence of formation of corrosion products at the coating/substrate interface and lifted/damaged the coating, thus exposing the substrate to undergo further deterioration.

#### 4.3 Effect of exposure time on corrosion rate

The exposure time provides a greater tendency to alter the mechanism of the corrosion behavior of AISI 316 stainless steel. The time constants for each specimen during corrosion were quantified, and five different exposure times were assigned for each of the corrosion tests. Fig.9 illustrates the effect of the exposure time on the corrosion rate of the uncoated and HVOF sprayed iron based amorphous coatings on AISI 316 stainless steel, during immersion corrosion tests with pH value 7 and chloride ion concentration 2.5 M. From the Figure, it was clear that, the corrosion rate decreased with increasing exposure time. The highest corrosion rate is observed at the exposure time of 360 h. It proves that the initial corrosion product impeded the passage of corrosion medium and provided protection for the uncoated and coated samples.

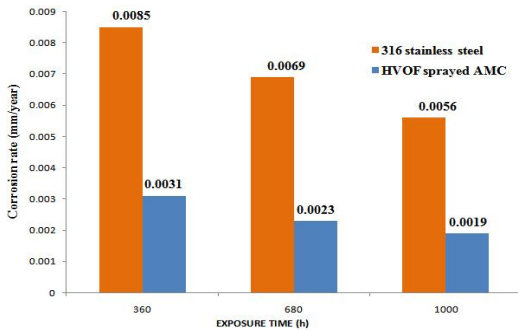


Fig. 9 Effect of exposure time on corrosion rate

In long time immersion with stainless steel dissolution and hydrogen evolution, the pH value of the solution will increase, namely basification. Basification should be propitious to the formation of passive film, which can protect the uncoated and coated samples. The insoluble corrosion products on the surface of the alloy could slow down the corrosion rate. The SEM micrographs of the corroded specimens after immersion corrosion test in NaCl solution with different exposure times depicted in Fig.9. At lower exposure times, a little amount of corrosion pits were observed on the surface

of the material as shown in Fig.10(a). At the higher exposure times, trench like cavities appear on the surface of stainless steel specimen Fig.10(c). It is clear from the Fig.10, localized corrosion associated with dense pitted areas showing lot of cracks on the surface of corrosion film for all the specimens tested. During the experiment, some black areas appeared initially, these areas become larger and additional similar areas appear with the increase in time. It was characterized by the observation of localized attack and many upheavals with pitting occurrence.

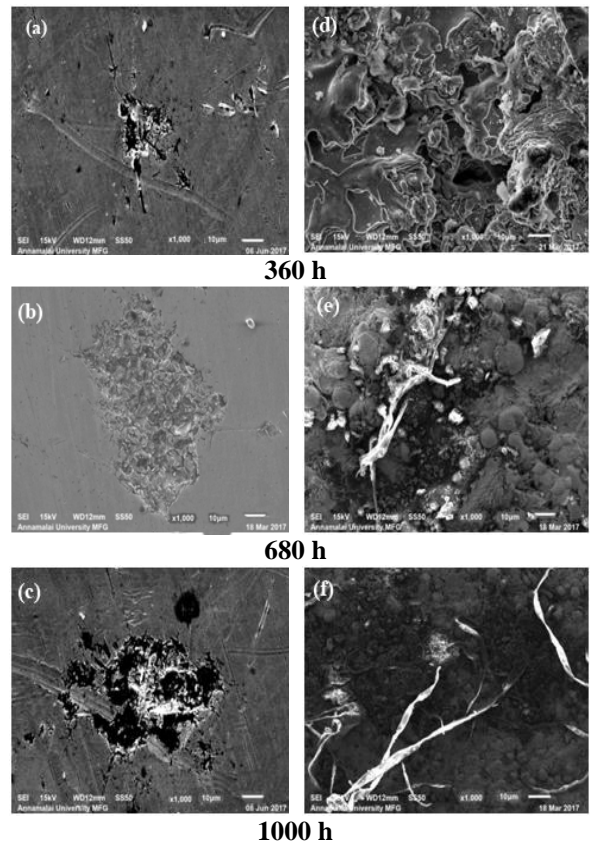


Fig. 10 Effect of exposure time on corrosion behavior of uncoated (a, b & c) and HVOF sprayed iron based amorphous coated specimens (d, e & f) after immersion corrosion test in NaCl solution

As shown in the SEM micrograph Fig.10(d), it can be seen that at lower immersion time coated specimen exhibits a slight degradation in these regions and the damage was confined primarily on the micro pores. At the higher immersion times, coating in exposed area was completely damaged, exposing the bright metal surface as presented in Fig.10(f).



## 5. Conclusion

(i) Empirical relationships were developed to predict the corrosion rate of uncoated and HVOF sprayed coatings on 316 stainless steel using response surface methodology. The developed relationship can be effectively used to predict the corrosion rate of uncoated and HVOF sprayed iron based amorphous coatings on 316 stainless steel at 95% confidence level.

(ii) The uncoated substrate and HVOF sprayed iron based amorphous coatings exhibited an increment in the corrosion resistance with the increase in pH. The corrosion rate was higher at the acidic media than the alkaline and neutral media with same concentrations and exposure time.

(iii) The uncoated and HVOF sprayed iron based amorphous coatings on 316 stainless steel corroded more seriously with the increase in Cl<sup>-</sup> concentrations. More the Cl<sup>-</sup> promoted the corrosion along with the rise in corrosion rate.

(iv) The corrosion resistance was formed in the uncoated and as coated samples with the increased exposure period. A corrosion resistivity prevails with the increase of immersion time, resulting with the formation of layer as a dominant factor to avoid the corrosion further.

## References

- Fang Luo, Andrew Cockburn, Martin Sparkes, Rocco Lupoi, Zhi-jun Chen, William Oneill, Jianhua Yao and Rong Liu (2015), "Performance characterization of Ni60WC coating on steel processed with supersonic laser deposition", *Def Tech*, Vol.11, 35-47.
- Wang Y, Xing ZZ, Luo Q, Rahman A, Jiao J, Qu SJ, Zheng YG and Shen J (2015), "Corrosion and erosion corrosion behaviour of activated combustion high-velocity air fuel sprayed Fe-based amorphous coatings in chloride-containing solutions", *Corros Sci.*, Vol. 98, 339-353.
- Zhou H, Zhang C, Wang W, Yasir M and Liu L (2015). "Microstructure and mechanical properties of Fe-based amorphous composite coatings reinforced by stainless steel powders", *J Mater. Sci Technol*, Vol.31, 43-47.
- Sasaki K, Burstein G T (2007), "Erosion Corrosion of stainless steel under impingement by a fluid jet", *Corros Sci*, Vol. 49, 92-102.
- Wang Y G, Zheng Y G, Ke W, Sun W H, Hou W L, Chag X C and Wang J Q (2011), "Slurry erosion corrosion behaviour of high-velocity oxy-fuel (HVOF) sprayed Fe based amorphous metallic coatings for marine pump in sand-containing NaCl solutions". *Corros Sci*, Vol. 53, 3177-3185.
- Rajahram S S, Harvey T J and Wood R J K (2009), "Erosion Corrosion resistance of engineering materials in various test conditions", *Wear*, Vol. 267, 244-254.
- Hu X and Neville A (2005), "The electrochemical response of stainless steels in liquid-solid impingement", *Wear*, Vol. 258, 641-648.
- Wang Y, L Jiang S, Zheng Y G, Ke W, Sun WH and Wang JQ (2011), "Effect of porosity sealing treatments on the corrosion resistance of high-velocity oxy-fuel (HVOF)-sprayed Fe- based amorphous metallic coatings", *Surf Coat Technol*. Vol.206, 1307-1318.
- Cherigui M, Feraoun H I, Feninehe N E, Aourag H and Coddet C (2004), "Structure of amorphous iron-based coatings processed by HVOF and APS thermally spraying", *Mater. Chem Phys*, Vol.85, 113-119.
- Bavaresco Sucharski Gustavo, Pukasiewicz Anderson Geraldo Marena, Vaz Rodolpho Fernando and Paredes Ramon Sigifredo Cortes (2015), "Optimization of the deposition parameters of HVOF FeMnCrSiPNiB thermally sprayed coatings", *Soldagem Inspecao*, Vol.20(2), 238-252.
- Vignesh S, Shanmugam K, Balasubramanian V and Sridhar K (2017), "Identifying the optimal HVOF spray parameters to attain minimum porosity and maximum hardness in iron based amorphous metallic coatings", *Defence Technology*, Vol.13, 101-110.
- Wu-Han Liu, Fuh-Sheng Shieu and Wei-Tien Hsiao (2014), "Enhancement of wear and corrosion resistance of iron-based hard coatings deposited by high-velocity oxygen fuel (HVOF) thermal spraying", *Surface & Coatings Technology*, Vol.249, 24-41.
- Zeng Z, Sakoda N, Tajiri T and Kuroda S (2008), "Structure and corrosion behavior of 316L stainless steel coatings formed by HVAF spraying with and without sealing", *Surface and Coatings Technology*, Vol.203(3), 284-290.
- ASTM G31-72, Standard Practices for Laboratory Immersion Corrosion Testing of Metals (2004), Vol 03.02.2004.
- Thirumalaikumarasamy D, Shanmugam K, Balasubramanian V and Kamal Jayaraj R (2017), "Multiobjective optimization of atmospheric plasma spray process parameters to deposit alumina coatings based on response surface", *Journal of Manufacturing Engineering*. Vol.12, Issue. 2, 82-93.
- Zhou Z, Wang L, Wang FC, Zhang HF, Liu YB and Xu SH (2009), "Formation and corrosion behavior of Fe-based amorphous metallic coatings by HVOF thermal spraying". *Surf Coat Technol*, Vol.204(5), 63- 70.
- Perry J M, Hodgkiess T and Neville A (2002), "A comparison of the corrosion behavior of WC-Co-Cr and WC-Co HVOF thermally sprayed coatings by in situ atomic force microscopy (AFM)", *Journal of thermal spray technology*, Vol.11(4), 536-541.
- Zhou Z, Wang L, Wang F C, Zhang H F, Liu Y B and Xu, S H (2007), Formation and corrosion behavior of Fe-based amorphous metallic coatings by HVOF thermal spraying. *Surf. Coat. Technol*. Vol. 48 (5), 1157.

19. Zeng, Z., Sakoda, N., Tajiri, T., and Kuroda, S. (2008). Structure and corrosion behavior of 316L stainless steel coatings formed by HVOF spraying with and without sealing. *Surface and Coatings Technology*, Vol.203(3), pp.284-290.
20. ASTM G31-72, *Standard Practices for Laboratory Immersion Corrosion Testing of Metals*, vol 03.02.2004 (2004).
21. Thirumalaikumarasamy, D, Shanmugam, K, Balasubramanian, V and Kamal Jayaraj, R. (2017), Multiobjective optimization of atmospheric plasma spray process parameters to deposit alumina coatings based on response surface. *Journal of Manufacturing Engineering*. Vol.12, Issue. 2, pp.82–93.
22. Zhou Z, Wang L, Wang FC, Zhang HF, Liu YB and Xu SH. (2009), Formation and corrosion behavior of Fe-based amorphous metallic coatings by HVOF thermal spraying. *Surf Coat Technol*, Vol.204(5), pp. 63- 70.
23. Perry, J. M., Hodgkiess, T. and Neville, A., (2002), A comparison of the corrosion behavior of WC-Co-Cr and WC-Co HVOF thermally sprayed coatings by in situ atomic force microscopy (AFM). *Journal of thermal spray technology*, Vol.11(4), pp.536-541.
24. Zhou, Z., Wang, L., Wang, F..C, Zhang, H.F., Liu, Y.B., and Xu, S.H. (2007), Formation and corrosion behavior of Fe-based amorphous metallic coatings by HVOF thermal spraying. *Surf. Coat. Technol*. Vol. 48(5), pp.1157.